FORMATION OF SHEAR INTERFEROGRAMS WITH DIFFUSELY SCATTERED FIELDS AND DOUBLE EXPOSURE RECORDING OF A GABOR HOLOGRAM OF A FOCUSED IMAGE OF AN AMPLITUDE SCREEN. PART I

V.G. Gusev

Tomsk State University
Received March 6, 1995

The shear interferometer is analyzed using records of a hologram of a focused image of an amplitude screen. It is demonstrated that spatial filtration of a diffraction field leads to formation of an interferogram bearing information about spherical aberrations of a lens with a doubled sensitivity.

As was shown in Refs. 1 and 2 shear interferograms are being formed in the bands of infinite width in the case of double exposure recording of a hologram of a focused image of a matt glass screen based on superposition of subjective speckle fields of two exposures in the plane of the hologram. Moreover, the interference pattern characterizing wave aberrations of a lens or an objective under control at the recording stage and the interference pattern characterizing aberrations of the optical systems in the channels of coherent radiation wave front for illuminating a matted glass screen and formation of an off-axis reference wave are localized in different planes. This makes it possible to obtain independent information about wave aberrations of an object under control by spatial filtration of the diffraction field at the stage of hologram reconstruction in its plane.

In this paper, we analyze specific features of shear interferogram formation at a double exposure recording of the Gabor hologram of a focused image of an amplitude screen in diffusely scattered fields.

According to Fig. 1*a* the amplitude screen *1* lying in the plane (x_1, y_1) is illuminated with a coherent radiation having a converging quasi-spherical wave front with a radius of curvature $R \le l_1$ where l_1 is the distance between the screen and the principal plane (x_2, y_2) of the lens L_1. By this lens, the real image of the screen is built in the plane of a photographic plate *2*. The Gabor hologram is recorded during the first exposure. Prior to second exposure, the amplitude screen and the plate are displaced. For instance, the screen is displaced along the x axis by a value a, and the plate is displaced opposite by the distance $b = a/\mu_1$ where $\mu_1 = l_1/l_2$ is the scale transformation factor, l_2 is the distance from the principal plane of the lens L_1 to the plate.

After the photographic processing, the coherent plane wave from a light source used at the stage of recording comes to the recorded double exposure Gabor hologram and an interference pattern is detected in the Fourier plane *3* (Fig. 1*b*).

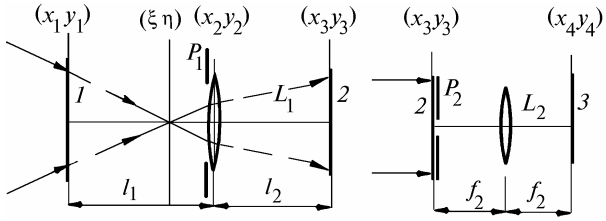

a *b*

FIG. 1. Optical arrangement for recording (a) and reconstruction (b) of a double exposure hologram of a focused image of an amplitude screen: 1 is the amplitude screen, 2 is the photographic plate hologram, 3 is the plane of detecting the interference pattern, L_1, L_2 are lenses, P_1 is the aperture diaphragm; P_2 is the spatial filter.

Based on discussion from Ref. 3, the distribution of the complex amplitude of the field in the first exposure takes the form

$$u_1(\xi, \eta) - \exp\left[\frac{ik}{2R}(\xi^2 + \eta^2)\right] F\left[\frac{k\xi}{R}, \frac{k\eta}{R}\right], \qquad (1)$$

in the plane (ξ, η) at the distance R from the screen. Here k is the wave number, $F\left[\frac{k\xi}{R}, \frac{k\eta}{R}\right] =$

$$= \int_{-\infty}^{\infty}\int [1 - t(x_1,y_1)]\exp i\varphi_0(x_1,y_1)\ \exp\left[-\frac{ik}{R}(x_1\xi + y_1\eta)\right] \times$$

$\times\, dx_1\, dy_1$ is the Fourier transform of the input function $[1 - t(x_1, y_1)]\ \exp i\,\varphi_0(x_1, y_1)$, $1 - t(x_1, y_1)$ is the screen transmission amplitude which is a random function of coordinates, $\varphi_0(x_1, y_1)$ is a determined function characterizing phase distortions of the radiation wave front irradiating the amplitude screen. The distortions are caused by aberrations of the optical system forming the wave front.

As follows from Eq. (1), the phase distribution of a diverging spherical wave with a radius of curvature R is superposed on the distribution of the field as a Fourier transform of the input function in the plane

0235-6880/97/02 89-08 $02.00

(ξ, η). According to Ref. 4, one can assume that the complex amplitude distribution of a real screen image in the plane (x_3, y_3) is a result of one more Fourier transformation performed with the lens L_1. Actually, since $\frac{1}{R}+\frac{1}{l_1-R}-\frac{M}{(l_1-R)^2}=0$ where $\frac{1}{M}=\frac{1}{l_1-R}-\frac{1}{f_1}+\frac{1}{l_2}$, f_1 is the focal length of the lens L_1, we have

$$u_1(x_3, y_3) \sim \exp\left[\frac{ik}{2l_2}(x_3^2+y_3^2)\right]\left\{\exp\left[-\frac{ikM}{2l_2^2}(x_3^2+y_3^2)\right]\times\right.$$

$$\left.\times F\left[\frac{kx_3M}{(l_1-R)l_2}, \frac{ky_3M}{(l_1-R)l_2}\right]\otimes P_1(x_3, y_3)\right\}, \qquad (2)$$

where $\otimes$ denotes convolution, $F\left[\frac{kx_3M}{(l_1-R)l_2}, \frac{ky_3M}{(l_1-R)l_2}\right]=$ $=\int_{-\infty}^{\infty}\int F\left[\frac{k\xi}{R}, \frac{k\eta}{R}\right]\exp\left[-\frac{ik(\xi x_3+\eta y_3)M}{(l_1-R)l_2}\right]d\xi d\eta$ is the Fourier transform of the integrand, $P_1(x_3, y_3) =$ $=\int_{-\infty}^{\infty}\int p_1(x_2, y_2)\exp i\,\varphi_1(x_2, y_2)\exp\left[-\frac{ik(x_2x_3+y_2y_3)}{l_2}\right]\times$ $\times\, dx_2dy_2$ is the Fourier transform of the distribution $p_1(x_2, y_2)\exp i\varphi_1(x_2, y_2)$ describing the pupil of the lens L_1 (Ref. 5). By this distribution, we take into account axial wave aberrations of the lens.

By two sequential Fourier transformations, we obtain

$$u_1(x_3, y_3) \sim \exp\left[\frac{ik}{2l_2}(x_3^2+y_3^2)\right]\times$$

$$\times\left\{\exp\left[-\frac{ik\mu_1(l_1-R)}{2Rl_2}(x_3^2+y_3^2)\right][1-t(-\mu_1x_3, -\mu_1y_3)]\times\right.$$

$$\left.\times\exp i\varphi_0(-\mu_1x_3, -\mu_1y_3)\otimes P_1(x_3, y_3)\right\}. \qquad (3)$$

The width of the function $P_1(x_3, y_3)$ is of $\lambda l_2/d$ (Ref. 6) where λ is the wavelength of light used for recording and reconstruction of the hologram, d is the pupil diameter of the lens L_1. So we can assume that the change of the phase of the spherical wave with a radius of curvature $Rl_2/(l_1-R)\mu_1$ does not exceed π within its domain. Then, let us remove the quadratic phase factor $\exp[-ik(x_3^2+y_3^2)(l_1-R)\mu_1/2Rl_2]$ out from the integral sign of the convolution with the function $P_1(x_3, y_3)$ in Eq. (3) for the region with the diameter $\le dR/(l_1-R)\mu_1$ in the plane (x_3, y_3) we obtain

$$u_1(x_3, y_3) \sim \exp\left[ik\frac{(Rl_2-l_1^2+Rl_1)}{2Rl_2^2}(x_3^2+y_3^2)\right]\times$$

$$\times\left\{[1-t(-\mu_1x_3, -\mu_1y_3)]\times\right.$$

$$\left.\times\exp i\varphi_0(-\mu_1x_3, -\mu_1y_3)\otimes P_1(x_3, y_3)\right\}. \qquad (4)$$

It follows from Eq. (4) that, by because of spatially limited scattered field, by the aperture of the lens L_1, every point of the amplitude screen image is broadened up to the dimensions of a subjective speckle defined by the width of the function $P_1(x_3, y_3)$ which is the result of diffraction of a plane wave on the pupil of the lens L_1. Besides, the distribution of phase distortions of the wave irradiating the screen is superposed on the subjective speckle field under the assumption that the period of the function $\varphi_0(-\mu_1x_3, -\mu_1y_3)$ exceeds the dimension of the subjective speckle. The phase distributions of the converging spherical wave for $R < l_1^2/(l_1+l_2)$, and diverging spherical wave for $l_1^2/(l_1+l_2) < R \le l_1$ are also superposed on it, and the quadratic phase factor is absent in Eq. (4) for $R = l_1^2/(l_1+l_2)$.

Let us write the expression for the complex amplitude of the field in the plane of the photographic plate before the second exposure:

$$u_2(x_3, y_3) \sim \exp\left\{\frac{ik(Rl_2-l_1^2+Rl_1)}{2Rl_2^2}[(x_3+b)^2+y_3^2]\right\}\times$$

$$\times\left\{[1-t(-\mu_1x_3, -\mu_1y_3)]\exp i\varphi_0(-\mu_1x_3-\mu_1b, -\mu_1y_3)\otimes\right.$$

$$\left.\otimes\exp\left[\frac{ikx_3b\mu_1(l_1-R)}{Rl_2}\right]P_1(x_3, y_3)\right\}. \qquad (5)$$

Let the photosensitive layer exposed to the light with the intensity $I(x_3, y_3) = u_1(x_3, y_3)u_1^*(x_3, y_3) + u_2(x_3, y_3)u_2^*(x_3, y_3)$ be processed within the linear portion of its characteristic curve of blackening. Then, taking into account the condition $t(x_1, y_1) << 1$ (Ref. 7) the transmission $\tau(x_3, y_3)$ of the photographic plate in Fig. 1*b* for the diffusely scattered component of light is defined by the expression

$$\begin{aligned}\tau(x_3, y_3) \sim & [\exp i\varphi_0(-\mu_1x_3, -\mu_1y_3)\otimes P_1(x_3, y_3)]\,[t(-\mu_1x_3, -\mu_1y_3)\exp -i\varphi_0(-\mu_1x_3, -\mu_1y_3)\otimes P_1^*(x_3, y_3)] + \\ & + [\exp -i\varphi_0(-\mu_1x_3, -\mu_1y_3)\otimes P_1^*(x_3, y_3)]\,[t(-\mu_1x_3, -\mu_1y_3)\exp i\varphi_0(-\mu_1x_3, -\mu_1y_3)\otimes P_1(x_3, y_3)] + \\ & + \left[\exp i\varphi_0(-\mu_1x_3-\mu_1b, -\mu_1y_3)\otimes\exp\left[\frac{ikx_3b\mu_1}{Rl_2}(l_1-R)\right]P_1(x_3, y_3)\right]\times \\ & \times\left[t(-\mu_1x_3, -\mu_1y_3)\exp -i\varphi_0(-\mu_1x_3-\mu_1b, -\mu_1y_3)\otimes\exp\left[-\frac{ikx_3b\mu_1(l_1-R)}{Rl_2}\right]P_1^*(x_3, y_3)\right] + \\ & + \left[\exp -i\varphi_0(-\mu_1x_3-\mu_1b, -\mu_1y_3)\otimes\exp\left[\frac{-ikx_3b\mu_1(l_1-R)}{Rl_2}\right]P_1^*(x_3, y_3)\right]\times \\ & \times\left[t(-\mu_1x_3, -\mu_1y_3)\exp i\varphi_0(-\mu_1x_3-\mu_1b, -\mu_1y_3)\otimes\exp\left[\frac{ikx_3b\mu_1(l_1-R)}{Rl_2}\right]P_1(x_3, y_3)\right]. \qquad (6)\end{aligned}$$

To reconstruct the double exposure Gabor hologram, according to Fig. 1*b*, the distribution of the field amplitude in the back focal plane of the lens L_2 with the focal length f_2 can be represented in the form[8]

$$u(x_3, y_3) \int_{-\infty}^{\infty}\int \tau(x_3, y_3)\exp\left[-\frac{ik}{f_2}(x_3 x_4 + y_3 y_4)\right] \times$$

$$\times \, dx_3 \, dy_3 \otimes P_2(x_4, y_4), \qquad (7)$$

where $P_2(x_3, y_3) = \int_{-\infty}^{\infty}\int p_2(x_3, y_3)\exp\left[-\frac{ik}{f_2}(x_3x_4 + y_3y_4)\right] \times$

$\times \, dx_3 dy_3$ is the Fourier transform of the transmission function of an opaque screen with a circular aperture.[9]

By substituting Eq. (6) into Eq. (7), we obtain

$$u(x_4, y_4) \sim \left\{\left[F_1(x_4, y_4)p_1(\mu_2 x_4, \mu_2 y_4) \times \right.\right.$$

$$\times \exp i\varphi_1(-\mu_2 x_4, -\mu_2 y_4)\Big]\otimes\Big\{\Big[F(x_4, y_4)\otimes$$

$$\otimes F_2(x_4, y_4)\Big]p_1(\mu_2 x_4, \mu_2 y_4)\exp -i\varphi_1(\mu_2 x_4, \mu_2 y_4)\Big\} +$$

$$+ \left[F_2(x_4, y_4)p_1(\mu_2 x_4, \mu_2 y_4)\exp -i\varphi_1(\mu_2 x_4, \mu_2 y_4)\right]\otimes$$

$$\otimes\Big\{\Big[F(x_4, y_4)\otimes F_1(x_4, y_4)\Big]\, p_1(\mu_2 x_4, \mu_2 y_4) \times$$

$$\times \exp i\varphi_1(-\mu_2 x_4, -\mu_2 y_4)\Big\} + \Big[F_3(x_4, y_4) \times$$

$$\times \, p_1\Big(\mu_2 x_4 - \frac{b\mu_1(l_1-R)}{R}, \, \mu_2 y_4\Big) \times$$

$$\times \exp i\varphi_1\Big(-\mu_2 x_4 + \frac{b\mu_1(l_1-R)}{R}, -\mu_2 y_4\Big)\Big] \otimes$$

$$\otimes\left\{\Big[F(x_4, y_4)\otimes F_4(x_4, y_4)\Big]p_1\Big(\mu_2 x_4 + \frac{b\mu_1(l_1-R)}{R}, \mu_2 y_4\Big) \times\right.$$

$$\left.\times \exp -i\varphi_1\Big(\mu_2 x_4 + \frac{b\mu_1(l_1-R)}{R}, \, \mu_2 y_4\Big)\right\} +$$

$$+ \Big[F_4(x_4, y_4)p_1\Big(\mu_2 x_4 + \frac{b\mu_1(l_1-R)}{R}, \, \mu_2 y_4\Big) \times$$

$$\times \exp -i\varphi_1\Big(\mu_2 x_4 + \frac{b\mu_1(l_1-R)}{R}, \mu_2 y_4\Big)\Big]\otimes$$

$$\otimes\Big\{\Big[F(x_4, y_4)\otimes F_3(x_4, y_4)\Big]p_1\Big(\mu_2 x_4 - \frac{b\mu_1(l_1-R)}{R}, \mu_2 y_4\Big)\times$$

$$\left.\times\exp i\varphi_1\Big(-\mu_2 x_4 + \frac{b\mu_1(l_1-R)}{R}, -\mu_2 y_4\Big)\Big\}\right\}\otimes P_2(x_4, y_4), \quad (8)$$

where $\mu_2 = l_2/f_2$ is the factor of scale transformation;

$$F(x_4, y_4) = \int_{-\infty}^{\infty}\int t(-\mu_1 x_3, -\mu_1 y_3)\exp\left[-\frac{ik(x_3 x_4 + y_3 y_4)}{f_2}\right] \times$$

$\times \, dx_3 \, dy_3$ is the Fourier transform of the absorption function of the amplitude screen in the plane of its image; F_1, F_2, F_3, F_4 are Fourier transforms of the functions $\exp i\varphi_0(-\mu_1 x_3, -\mu_1 y_3)$, $\exp -i\varphi_0(-\mu_1 x_3, -\mu_3 y_3)$, $\exp i\varphi_0(-\mu_1 x_3 - \mu_1 b, -\mu_1 y_3)$, $\exp -i\varphi_0(-\mu_1 x_3 - \mu_1 b, -\mu_1 y_3)$ respectively to the scale $(kx_4/f_2, \, ky_4/f_2)$.

Since the domains of the functions F_1, F_2, F_3, F_4 are small, one can put $F_1 = F_2 = F_3 = F_4 = \delta(x_4, y_4)$ where $\delta(x_4, y_4)$ is the Dirac delta function. Then the expression (8) takes the form

$$u(x_4, y_4) \sim \Big[\exp -i\varphi_1(\mu_2 x_4, \mu_2 y_4) + \exp i\varphi_1(-\mu_2 x_4, -\mu_2 y_4) +$$

$$+ \exp -i\varphi_1\Big(\mu_2 x_4 + \frac{b\mu_1(l_1-R)}{R}, \, \mu_2 y_4\Big) +$$

$$+ \exp i\varphi_1\Big(-\mu_2 x_4 + \frac{b\mu_1(l_1-R)}{R}, \, -\mu_2 y_4\Big)\Big] \times$$

$$\times \, F(x_4, y_4)\otimes P_2(x_4, y_4). \qquad (9)$$

within the overlap area of the pupil functions where the subjective speckles of two exposures coincide.

If the dimension of the subjective speckle defined by the width of the function $P_2(x_4, y_4)$ in the observation is less than the period of the phase function modulating the speckle field and standing between the brackets in Eq. (9) at least by an order of magnitude,[10] one can remove the function out from the convolution integral. In view of the evens of the function $\varphi_1(x_2, y_2)$, the superposition of the correlating speckle fields of the two exposures leads to the following illumination distribution

$$I(x_4, y_4) \sim \left[1 + \cos 2\varphi_1(\mu_2 x_4, \, \mu_2 y_4)\right] \times$$

$$\times \left[1 + \cos \frac{\partial\varphi_1(\mu_2 x_4, \, \mu_2 y_4)}{\partial\mu_2 x_4}\,\frac{b\mu_1(l_1-R)}{R}\right] \times$$

$$\times \, |F(x_4, y_4)\otimes P_2(x_4, y_4)|^2, \qquad (10)$$

where

$$\frac{\partial\varphi_1(\mu_2 x_4, \, \mu_2 y_4)}{\partial\mu_2 x_4}\,\frac{b\mu_1(l_1-R)}{R} = \varphi_1\Big(\mu_2 x_4 + \frac{b\mu_1(l_1-R)}{R}, \mu_2 y_4\Big) -$$

$$- \varphi_1(\mu_2 x_4, \, \mu_2 y_4).$$

As follows from Eq. (10), the subjective speckle structure is modulated by interference fringes in the observation plane (see Fig. 1*b*). The interference pattern characterizes the spherical aberration of the lens L_1 (see Fig. 1*a*). Its shape is a result of combination of two types of interference patterns, namely, the interference pattern as a shear interferogram in bands of infinite width and interference pattern in bands of equal thickness. Besides, the interference pattern in bands of equal thickness is also formed at a single exposure of a photographic plate (as it follows from Eq. (9)) and has double sensitivity of the interferometer to the spherical aberration of the lens L_1. As to the sensitivity of the shear interferometer, it is determined by the displacement b and the geometrical factor $G = \mu_1(l_1 - R)/R$. For $l_1 = R$, the sensitivity equals zero as the relative inclination angle $\beta = \dfrac{b\mu_1(l_1 - R)}{R\, l_2}$ between the speckle fields of two exposures in the plane of the photographic plate is zero, as it follows

from Eqs. (4) and (5). With the decrease in the value R as compared with l_1, the sensitivity of the interferometer increases due to the geometrical factor for a fixed value of b. When $R = l_1^2/(l_1 + l_2)$, the sensitivity of the interferometer is determined only by the value of the lateral displacement b.

Let the regular transmission component of the amplitude screen overlap the pupil of the lens L_1 after focusing on the plane (ξ, η) (see Fig. 1*a*) at the hologram of a focused image. Then one should use the general expressions for complex field amplitudes corresponding to the first and second exposures in the plane of the photographic plate

$$u_1'(x_3, y_3) \sim \exp\left[\frac{ik}{2l_2}(x_3^2 + y_3^2)\right] \times$$
$$\times \left\{\exp\left[-\frac{ik\mu_1(l_1 - R)}{2Rl_2}(x_3^2 + y_3^2)\right][1 - t(\mu_1 x_3, -\mu_1 y_3)] \times\right.$$
$$\left.\times \exp i\varphi_0(-\mu_1 x_3, -\mu_1 y_3) \otimes P_1(x_4, y_4)\right\}, \qquad (11)$$

$$u_2'(x_3, y_3) \sim \exp\left[\frac{ik}{2l_2}(x_3^2 + y_3^2)\right] \exp\left(ik\frac{Rl_2 - l_1^2 + Rl_1}{Rl_2^2} x_3 b\right) \times$$
$$\times \left\{\exp\left[-\frac{ik\mu_1(l_1 - R)}{2Rl_2}(x_3^2 + y_3^2)\right][1 - t(-\mu_1 x_3, -\mu_1 y_3)] \times\right.$$
$$\left.\times \exp i\varphi_0(-\mu_1 x_3 - \mu_1 b, -\mu_1 y_3) \otimes\right.$$
$$\left.\otimes \exp\left[\frac{ikx_3 b\mu_1(l_1 - R)}{Rl_2}\right] P_1(x_3, y_3)\right\} \qquad (12)$$

in spatial filtration of the diffraction field off the hologram plane (Fig. 2) at the stage of its reconstruction for determining the transmission of the double exposure hologram.

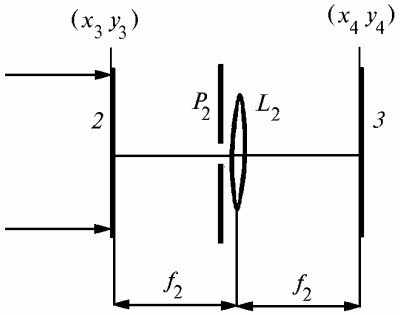

FIG. 2. Scheme of detection of the interference pattern in filtration in the near zone of diffraction

Based on the assumptions that the period of the function $\varphi_0(-\mu_1 x_3, -\mu_1 y_3)$ exceeds the dimension of the subjective speckle in the plane of the photographic plate, $t(x_1, y_1) \ll 1$, and the negative is processed within the linear portion of its characteristic curve, we write the transmission amplitude $\tau'(x_3, y_3)$ of the double exposure

$$\tau'(x_3, y_3) \sim \left\{\exp\left[-\frac{ik\mu_1(l_1 - R)}{2Rl_2}(x_3^2 + y_3^2)\right] \otimes P_1(x_3, y_3)\right\} \left\{t(-\mu_1 x_3, -\mu_1 y_3) \exp\left[\frac{ik\mu_1(l_1 - R)}{2Rl_2}(x_3^2 + y_3^2)\right] \otimes P_1^*(x_3, y_3)\right\} +$$
$$+ \left\{\exp\left[\frac{ik\mu_1(l_1 - R)}{2Rl_2}(x_3^2 + y_3^2)\right] \otimes P_1^*(x_3, y_3)\right\} \left\{t(-\mu_1 x_3, -\mu_1 y_3) \exp\left[\frac{-ik\mu_1(l_1 - R)}{2Rl_2}(x_3^2 + y_3^2)\right] \otimes P_1(x_3, y_3)\right\} +$$
$$+ \left\{\exp\left[\frac{-ik\mu_1(l_1 - R)}{2Rl_2}(x_3^2 + y_3^2)\right] \otimes \exp\left[\frac{ikx_3 b\mu_1(l_1 - R)}{Rl_2}\right] P_1^*(x_3, y_3)\right\} \times$$
$$\times \left\{t(-\mu_1 x_3, -\mu_1 y_3) \exp\left[\frac{ik\mu_1(l_1 - R)}{2Rl_2}(x_3^2 + y_3^2)\right] \otimes \exp\left[\frac{-ikx_3 b\mu_1(l_1 - R)}{Rl_2}\right] P_1^*(x_3, y_3)\right\} +$$
$$+ \left\{\exp\left[\frac{ik\mu_1(l_1 - R)}{2Rl_2}(x_3^2 + y_3^2)\right] \otimes \exp\left[\frac{-ikx_3 b\mu_1(l_1 - R)}{Rl_2}\right] P_1^*(x_3, y_3)\right\} \times$$
$$\times \left\{t(-\mu_1 x_3, -\mu_1 y_3) \exp\left[\frac{-ik\mu_1(l_1 - R)}{2Rl_2}(x_3^2 + y_3^2)\right] \otimes \exp\left[\frac{ikx_3 b\mu_1(l_1 - R)}{Rl_2}\right] P_1(x_3, y_3)\right\}, \qquad (13)$$

Gabor hologram in Fig. 2 in the form omitting the regular transmission component of light because it determines the illumination distributions in the observation plane only in a small spot.

Then the complex amplitude distribution of a diffusely scattered component of the field in the back focal plane of the lens L_2 (Fig. 2) is defined by the expression for the maximal value of the correlation functions.

$$u'(x_4, y_4) \sim \left\{\left\{\exp\left[\frac{ikR\mu_2}{2\mu_1(l_1 - R)f_2}(x_4^2 + y_4^2)\right] p_1(\mu_2 x_4, \mu_2 y_4) \exp i\varphi_0(-\mu_2 x_4, -\mu_2 y_4)\right\} \otimes\right.$$

$$\otimes\left\{\left[F(x_4,y_4)\otimes\exp\left[\frac{-ikR\mu_2}{2\mu_1(l_1-R)f_2}(x_4^2+y_4^2)\right]\right]p_1(\mu_2x_4,\mu_2y_4)\exp-i\varphi_1(\mu_2x_4,\mu_2y_4)\right\}+$$

$$+\left\{\exp\left[\frac{-ikR\mu_2}{2\mu_1(l_1-R)f_2}(x_4^2+y_4^2)\right]p_1(\mu_2x_4,\mu_2y_4)\exp-i\varphi_1(\mu_2x_4,\mu_2y_4)\right\}\otimes$$

$$\otimes\left\{\left[F(x_4,y_4)\otimes\exp\left[\frac{ikR\mu_2}{2\mu_1(l_1-R)f_2}(x_4^2+y_4^2)\right]\right]p_1(\mu_2x_4,\mu_2y_4)\exp i\varphi_1(-\mu_2x_4,-\mu_2y_4)\right\}+$$

$$+\left\{\exp\left[\frac{ikR\mu_2}{2\mu_1(l_1-R)f_2}(x_4^2+y_4^2)\right]p_1\left[\mu_2x_4-\frac{b\mu_1(l_1-R)}{R},\mu_2y_4\right]\exp\ i\varphi_1\left[-\mu_2x_4+\frac{b\mu_1(l_1-R)}{R},-\mu_2y_4\right]\right\}\otimes$$

$$\otimes\left\{\left[F(x_4,y_4)\otimes\exp\left[\frac{-ikR\mu_2}{2\mu_1(l_1-R)f_2}(x_4^2+y_4^2)\right]\right]p_1\left[\mu_2x_4+\frac{b\mu_1(l_1-R)}{R},\mu_2y_4\right]\exp-i\varphi_1\left[\mu_2x_4+\frac{b\mu_1(l_1-R)}{R},-\mu_2y_4\right]\right\}+$$

$$+\left\{\exp\left[\frac{-ikR\mu_2}{2\mu_1(l_1-R)f_2}(x_4^2+y_4^2)\right]p_1\left[\mu_2x_4+\frac{b\mu_1(l_1-R)}{R},\mu_2y_4\right]\exp-i\varphi_1\left[\mu_2x_4+\frac{b\mu_1(l_1-R)}{R},\mu_2y_4\right]\right\}\otimes$$

$$\otimes\left\{\left[F(x_4,y_4)\otimes\exp\left[\frac{ikR\mu_2}{2\mu_1(l_1-R)f_2}(x_4^2+y_4^2)\right]\right]p_1\left[\mu_2x_4-\frac{b\mu_1(l_1-R)}{R},\mu_2y_4\right]\exp i\varphi_1\left[-\mu_2x_4+\frac{b\mu_1(l_1-R)}{R},-\mu_2y_4\right]\right\}\otimes P_2(x_4,y_4). \tag{14}$$

With regard to the fact that $\exp\left[\frac{-ikR\mu_2}{2\mu_1(l_1-R)f_2}(x_4^2+y_4^2)\right]\otimes\exp\left[\frac{ikR\mu_2}{2\mu_1(l_1-R)f_2}(x_4^2+y_4^2)\right]=\delta(x_4,\ y_4)$ (Ref. 11), the expression (14) takes the form

$$u'(x_4,\ y_4)\sim\left\{1+\exp-i\left[\frac{\partial\varphi_1(\mu_2x_4,\ \mu_2y_4)}{\partial\mu_2x_4}\frac{2b\mu_1(l_1-R)}{R}\right]\right\}F(x_4,\ y_4)\otimes P_2(x_4,\ y_4). \tag{15}$$

By virtue of the above–stated assumption that the dimension of the subjective speckle in the observation plane $(x_4,\ y_4)$ (see Fig. 2) is small as compared with the period of the phase function modulating the speckle field, the superposition of correlating speckle fields of two exposures leads to the following illumination distribution

$$I'(x_4,y_4)\sim\left[1+\cos\frac{\partial\varphi_1(\mu_2x_4,\ \mu_2y_4)}{\partial\mu_2x_4}\frac{2b\mu_1(l_1-R)}{R}\right]\times$$

$$\times\ |F(x_4,\ y_4)\otimes P_2(x_4,\ y_4)|^2. \tag{16}$$

As follows from expression (16), the subjective speckle structure is modulated by interference fringes. The interference pattern has the shape of a shear interferogram in the bands of infinite width. Moreover, the sensitivity of the interferometer for fixed values if the geometrical factor and lateral displacement is twice as large.

In the experiment, double exposure Gabor holograms of the focused image of the amplitude screen were recorded on Mikrat YRL plates using a He-Ne-laser operating at the wavelength of 0.63 μm.

As an example, Fig. 3*a* presents an interference pattern in bands of equal thickness. It characterizes spherical aberration of a lens with the focal length $f_1 = 160$ mm, pupil diameter $d = 27$ mm. The recording of the hologram was performed using the lens for a unit magnification with $R = l_1$ in the plane of the paraxial image of the amplitude screen with a single exposure. To provide vignetting of the spatial wave spectrum, the diameter of the illuminated part of the amplitude screen was 35 mm. The detection of the interference pattern with an objective having focal length $f_2 = 80$ mm (see Fig. 1*b*) did not require spatial filtration of the diffraction field in the hologram plane. This is explained by the fact that the conditions of spatial invariance of the pulse response of the lens L_1 (Ref. 12) are satisfied on all its aperture for the considered case of formation of the interference pattern in the bands of equal thickness in diffusely scattered fields. The spatial invariance of the pulse response of the lens for the Gabor hologram of a focused image of the amplitude screen manifests itself by the fact that quasiplane waves of (–1) and (+1) diffraction orders coincide in directions irregardless of whether the hologram is reconstructed at the point of the optical axis or out of it. When the value R decreases as compared with l_1, the condition of full isoplanatism of the optical system of image formation is violated and there appears an angle between diffracting waves of (–1) and (+1) diffraction orders. The angle increases when the radius of curvature of the wave front of coherent radiation illuminating the amplitude screen deviates from the distance between it and the principal plane of the lens controlled. In these cases, spatial filtration of the diffraction field in the hologram plane on the optical axis in Fig. 1*b* is required in order to detect the interference pattern in Fig. 3*a*.

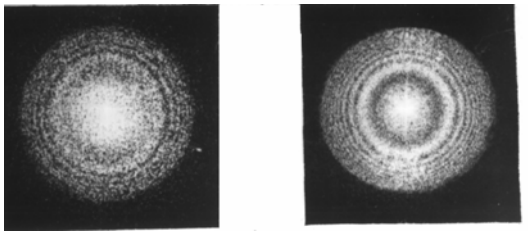

a *b*

FIG. 3. Interference patterns in the bands of equal thickness characterizing: a – spherical aberration of the lens controlled; b – spherical aberration and defocusing.

As with the classical Twyman–Green interferometer,[13] the interference pattern in the bands of equal thickness in Fig. 3*a* characterizes the double sensitivity of the interferometer to the spherical aberration of the lens. However, although the increase of sensitivity in the Twyman–Green interferometer occurs as a result of two-fold passage of a wave through an object controlled in the measurement channel, the mechanism of formation of an interference pattern in the bands of equal thickness is quite different in the considered case. As follows from Eq. (9), the fronts of quasiplane waves in (–1) and (+1) diffraction orders are faced each other and one of the fronts is inverted around the optical axis with respect to the other.

In the case of a single exposure recording of the Gabor hologram of a focused image of the amplitude screen when the photographic plate is displaced from the paraxial image plane by 1.15 mm, there is formed an interference pattern in the bands of equal thickness (Fig. 3*b*) characterizing the spherical aberration and defocusing of the lens L_1. Moreover, the spatial invariance of its pulse response is violated on all its aperture and, in order to detect the interference pattern, spatial filtration of the diffraction field in the hologram plane on the optical axis (see Fig. 1*b*) is required. A high–contrast interference pattern in Fig. 3*b* was observed for the filtering diaphragm diameter p_2 which does not exceed 6 mm.

Figure 4*a* presents the result of reconstruction of a double exposure Gabor hologram of a paraxial amplitude screen image focused by a lens controlled with unit magnification at the point $x_3' = 6$ mm, $y_3' = 0$ by a small-aperture (≈2 mm) laser beam. The hologram was recorded at $R = l_1/2$. Before the second exposure, the amplitude screen was displaced along the x axis by the value $a = (2.2 \pm 0.002)$ mm, and the photographic plate was displaced along the opposite direction by the value $b = (2.2 \pm 0.002)$ mm. Diffracting waves form shear interferograms in the bands of infinite width both in (–1) and (+1) diffraction orders. They characterize wave aberrations of the lens controlled, L_1, (see Fig. 1*a*) due to double exposure of the plate. Besides, in a small range of overlap of the wave fronts the superposition of waves in (–1) and (+1) diffraction orders leads to formation of an interference pattern caused by facing of the pair of the wave fronts and the turn around the optical axis by 180° with respect to the other pair (taking into account that there is an angle $\gamma = x_3'/l$ ($l = l_1 = l_2$) between the waves in (–1) and (+1) diffraction orders. The interference pattern presented in Fig. 4*b* and described by the expression (10) is formed in the observation plane (see Fig. 1*b*) in reconstruction of the hologram by a small-aperture laser beam at a point of the optical axis when $\gamma = 0$ and the waves in (–1) and (+1) diffraction orders coincide in direction.

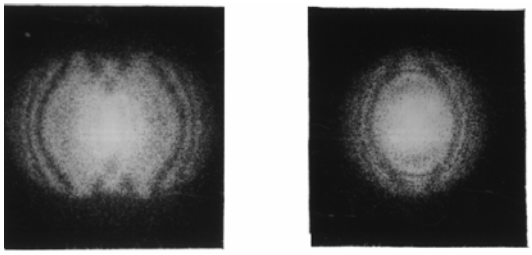

a *b*

FIG. 4. Interference patterns detected in spatial filtration of the diffraction field in the hologram plane: a – off the optical axis; b – on the optical axis.

If the double exposure hologram considered of the focused image of the amplitude screen is then reconstructed according to Fig. 2, a shear interferogram in the bands of infinite width is formed in the observation plane (x_4, y_4) in spatial filtration of the diffraction field on the optical axis off the hologram plane (the diameter of the filtering aperture diaphragm p_2 of the lens L_2 was ≈2 mm). The interferogram is described by Eq. (16) and presented in Fig. 5 to a larger scale as compared with Fig. 4. As to Fig. 4*b*, the shear interferogram characterizes spherical aberration in the paraxial focus of the lens controlled but, in contrast to Fig. 4*b*, the sensitivity of the interferometer is twice as large for a fixed value of the lateral displacement b. The lens L_2 performs the Fourier transform of the field diffracting on the hologram both in Fig. 1*b* and Fig. 2. However, in the first case the interference pattern is formed on the optical axis as a result of spatial filtration of the field in its plane; the pattern corresponds to a small region of spatial frequencies of the amplitude screen bounded by the aperture of the controlled lens L_1. Moreover, the directions of corresponding spatial frequencies are close to the direction of the optical axis. In the second case, the whole range of spatial frequencies of the hologram of the focused amplitude screen image is detected, and filtration on the optical axis is necessary to record the spectra in (–1) and (+1) diffraction orders. Information about aberrations of the lens L_1 controlled is contained, as in Ref. 14, not only in the objective wave (diffusely scattered light component) but also in the reference wave (regular light transmission component completely overlapping with the pupil of the lens L_1). Since the high-frequency holographic interference fringes bear this information

within the whole hologram, this causes double sensitivity of the shear interferometer.

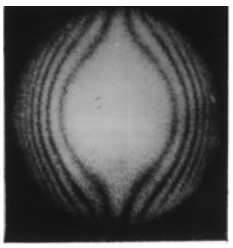

FIG. 5. Shear interferogram detected in the Fourier plane with spatial filtration of the diffraction field on the optical axis beyond the hologram plane.

To obtain non-zero sensitivity of the shear interferometer in the case of double exposure recording of the Gabor hologram of a focused image of an amplitude screen at $R = l_1$, one can use the well-known[2] particular method of superposing subjective speckle fields of two exposures in the plane of the photographic plate. In this case, before the second exposure, the amplitude screen is displaced, for instance, along the x axis by the value a, and the lens L_1 controlled is displaced by the shift $b = af_1/l_1$ along the same direction in its principal plane. One can demonstrate that the illumination distribution in the Fourier plane takes the form

$$I(x_4, y_4) \sim \{1 + \cos 2\varphi_1(\mu_2 x_4, \mu_2 y_4)\} \times$$
$$\times \left\{1 + \cos\left[\frac{\partial\varphi_1(\mu_2 x_4, \mu_2 y_4)}{\partial\mu_2 x_4} b\right]\right\} \times$$
$$\times |F(x_4, y_4) \otimes P_2(x_4, y_4)|^2. \qquad (17)$$

at the reconstruction state for the double exposure Gabor hologram of a focused image of the amplitude screen.

Figure 6 presents the interference pattern described by expression (17) and characterizing the spherical aberration of the lens L_1 controlled in the paraxial focus for the displacement $b = (2.4 \pm 0.002)$ mm. To detect it, spatial filtration of the diffraction field is not required.

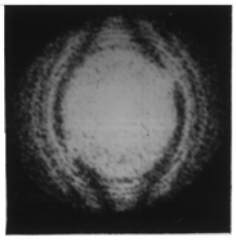

FIG. 6. Interference pattern corresponding to the double exposure recording of the hologram in the case of displacement of the screen and the lens before the second exposure.

It should be noted that the frequency of interference fringes grows with the decrease of focal length of the lens controlled and increase in defocusing (see Fig. 3*b*). If the period of interference fringes becomes comparable with the dimension of the subjective speckle, the visibility of the interference pattern in the bands of equal thickness is zero. Then one can exclude the first factor in Eqs. (10) and (17) and the double exposure recording of the Gabor hologram of a focused image of an amplitude screen leads to formation of low-frequency interference pattern of lateral displacement in spatial filtration of the diffraction field in the hologram plane at the stage of its reconstruction.

Thus, this study demonstrates that the double exposure recording of the Gabor hologram of a focused amplitude screen image provides for formation of the interference pattern insensitive to the off-axis wave aberration of the lens controlled as compared with the double exposure recording of the hologram of the focused image of a matt glass screen.[1,2] It can be explained by interference of counter waves whose fronts are turned by 180° to each other. Besides, the recording of the hologram in the plane of the paraxial image of the amplitude screen leads to formation of an interference pattern in the bands of equal thickness in diffusely scattered fields. The pattern characterizes the spherical aberration of the lens controlled with double sensitivity. Moreover, the sensitivity of the shear interferometer also increases twice for a fixed value of displacement in double exposure recording of the hologram under the condition that the pupil of the lens under control overlaps with the regular component of light transmission of the screen.

REFERENCES

1. V.G. Gusev, Atm. Opt. **3**, No. 10, 947–955 (1990).
2. V.G. Gusev, Atm. Opt. **4**, No. 3, 211–217 (1991).
3. R.J. Collier, C.B. Burckhardt, and L.H. Lin, *Optical Holography* (Academic Press, New York, 1971).
4. V.G. Gusev, Atm. Opt. **5**, No. 2, 73–78 (1992).
5. D. Goodman, *Introduction to Fourier Optics* (Mc Graw Hill, New York, 1968).
6. M. Francon, *Granularite Laser (Speckle) et ses Applications en Optique* (Masson, Paris, 1978).
7. D. Gabor, Nature **161**, 777–778 (1948).
8. V.G. Gusev, Opt. Spektrosk. **69**, No. 5, 1125–1128 (1990).
9. M. Born and E. Wolf, *Principles of Optics* (Pergamon Press, Oxford, 1970).
10. R. Jones and C. Wykes, *Holographic and Speckle Interferometry* (Cambridge University Press, 1986).
11. L.M. Soroko, *Foundations of Holography and Coherent Optics* (Nauka, Moscow, 1971), 601 pp.
12. S.M. Gorskii, V.A. Zverev, and A.Z. Matveew, Izv. Vyssh. Uchebn. Zaved. Ser. Radiofiz. **20**, No. 4, 522–527 (1977).
13. D. Malacara, ed., *Optical Shop Testing* (John Wiley and Sons, 1978).
14. V.G. Gusev, Atmos. Oceanic Opt. **10**, No. 1, 11–17 (1997).